Desalination and Water Treatment
www.deswater.com

doi: 10.5004/dwt.2020.25687

193 (2020) 106–116
July

Surface modification of TFC membranes using PVA and nanomaterials for enhancing fouling resistance

S.A. El-Behary[a,*], A.M. El-Aassar[a], M. Aboelfadl[a], Nevien Abdel-Atey[b], A.T. Kandil[b]

[a]*Desert Research Center, Hydro Geochemistry Department, Cairo, Egypt, Tel. +20 1017651764; email: shaimaa.awad@edrc.gov.eg (S.A. El-Behary)*
[b]*Faculty of Science, Helwan University, Cairo, Egypt*

Received 6 December 2019; Accepted 12 February 2020

ABSTRACT

Commercial thin-film composite aromatic polyamide reverse osmosis membranes were modified through the surface coating of polyvinyl alcohol with/without different nanomaterials to improve the commercial membrane fouling resistance. The surface characterization of both neat and modified membranes was carried out using different instruments such as attenuated total reflectance-Fourier transform infrared spectroscopy, X-ray diffraction, scanning electron microscopy, dynamic mechanical analysis, thermogravimetric analysis, and contact angle measurement. Also, the comparison between neat and different modified reverse osmosis membranes was achieved through water desalination processes at different operation conditions with different salt types. The obtained results were promising, indicating that the modified reverse osmosis membranes exhibited an increase in both the permeate flux and the salt rejection (%), as well as organic matter removal. The evaluation of membrane performance under different test conditions was carried out and compared with control, that is, unmodified neat membrane data. Surface modification has the potential to enable the use of existing thin-film composite membranes for all osmosis applications.

Keywords: Fouling resistance; Surface modification; Polyvinyl alcohol; Different nanomaterials

1. Introduction

With the rapidly increasing demands on water resources, the freshwater shortage has become an important issue affecting the economic and social development in many countries. As one of the main technologies for producing freshwater from saline water and other wastewater sources, reverse osmosis (RO) has been widely used so far. The reverse osmosis (RO) membrane of choice worldwide is the polyamide (PA) thin-film composite membrane. The PA composite membrane is made by forming a thin PA film on the finely porous surface of a polysulfone (PS) supporting membrane by an interfacial reaction between the reactant pair trimesoyl chloride and *m*-phenylenediamine.

Today, the membrane is commercially supplied. Although the membrane performance is excellent, major membrane deficiencies remain that contribute to fouling is considered the deterioration of the membrane surface properties due to accumulation of the particle on the surface or inside the pores of the membrane which lead to reduced membrane life and higher operating costs [1].

There are mainly four types of foulants in RO membrane fouling: inorganic (salt precipitations such as metal hydroxides and carbonates), organic (natural organic matters such as humic acid), colloidal (suspended particles such

* Corresponding author.

Presented at the 4th International Water Desalination Conference: Future of Water Desalination in Egypt and the Middle East, 24–27 February 2020, Cairo, Egypt

as silica) and biological (such as bacteria and fungi). Because RO membranes are nonporous, the formation of a fouling layer on the membrane surface is referred to as the dominant fouling mechanism. RO membrane fouling is closely related to the interaction between the membrane surface and the foulants [2].

Fouling is a complex problem, and it can be affected by a greater number of factors. In general, these factors can be classified into three groups as shown in Fig. 1.

The fouling groups can be classifying into:

- *Feed water characteristics*: membrane fouling is strongly dependent on the type of foulants present in the feed water, their concentrations, and their physicochemical properties (functional groups, charge, size, conformation, etc.).
- *Membrane properties*: membrane fouling can be significantly affected by membrane properties, such as surface roughness, charge properties, and hydrophobicity. In general, smooth, low surface charge, and more hydrophilic membranes tend to show better anti-fouling properties at the initial stage of membrane fouling.
- *Operational conditions*: Membrane fouling is strongly affected by hydrodynamic conditions such as flux and cross-flow velocity. In general, severe fouling can occur at higher membrane flux and/or lower cross-flow [3].

The membrane surface properties have been shown to play an important role in fouling resistance, membrane properties may affect fouling via (1) non-homogeneity and surface morphology (e.g., surface roughness), which affect both the hydrodynamic and the surface interaction near/at the liquid–membrane interface, (2) electro-static interaction, and (3) acid-base interaction [1].

Minimizing polymeric membrane fouling was considered the main approach toward the prevention of the undesired adsorption or adhesion processes on the surface of the membrane, because this will prevent or, at least, slow down the subsequent accumulation of colloids [4].

Anti-fouling RO membranes, which can improve the efficiency of the RO process for water treatment, have been obtained by changing the surface properties (roughness, hydrophilicity, and surface charge) of the aromatic polyamide thin-film composite RO membranes without impairing their transport characteristics [5,6]. Surface modification techniques such as surface coating [7,8], surface grafting [9,10], and surface hydrolysis [11,12] have been widely adopted to modify or tail or the surface properties of the aromatic polyamide thin-film composite RO membranes. It has been illustrated that surface coating is an efficient and simple technique for membrane surface modification; and that the proposed method for creating a fouling resistant RO membranes to apply a smooth coating of a hydrophilic and neutrally charged material such as polyvinyl alcohol (PVA), polydopamine, polyether–polyamide block copolymers, and poly(ethylene glycol) (PEG)-based materials on the surface of the commercial RO membrane [13,14].

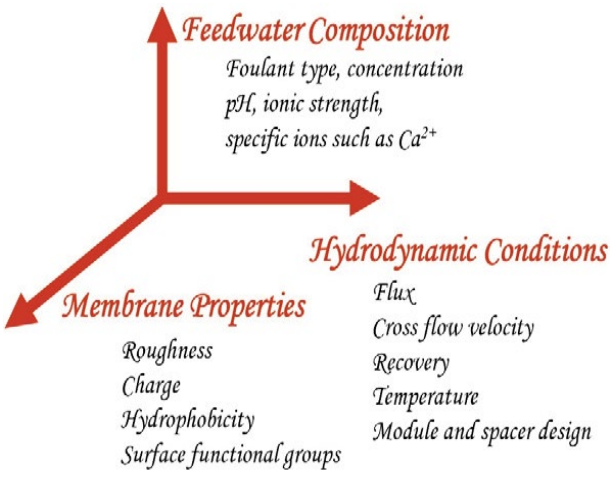

Fig. 1. Classification of fouling groups.

In particular polyvinyl alcohol polymer seems attractive for the preparation of membranes because of its high water permeability and good film-forming properties it's also known that polyvinyl alcohol is little affected by grease, hydrocarbons, and animal or vegetable oil, it has outstanding physical and chemical stability against organic solvents polyvinyl alcohol is readily soluble in water and no other solvent is necessary when used in RO, however, polyvinyl alcohol membranes are known to be poor in the rejection of salts so several attempts have been made to improve the selectivity by cross-linking the polyvinyl alcohol molecules with each other. Both di-aldehydes and dibasic acid were used as cross-linking agent [15].

Numerous techniques have been used to cross-link PVA and manufacture an ultra-thin film of cross-linked PVA, such as cross-linking by heat, radiation treatment, or treatment with organic compounds. PVA and a diamine compound have been used together as the polymeric precursor for manufacturing the thin-film desalting barrier of a composite membrane [16].

Nanomaterials have recently gained a considerable amount of attention because of their unique physical and chemical properties and their importance in technological applications. The rapid growth in nanotechnology has spurred significant interest in the environmental applications of nanomaterials. In particular, it's potential to revolutionize century-old conventional water treatment processes have been enunciated recently. Nanocomposites possess several advantages such as greater thermal stability, increased strength, enhanced electrical conductivity, improved flammability properties, etc. of the polymer matrix. Several nanomaterials, titanium dioxide, carbon nanotubes, silica, silver, and zinc oxide used to enhance the fouling resistance process.

The aim of the present work is to synthesis, characterization, and evaluation of the modified Polyamide/polyvinyl alcohol (PA/PVA) thin-film composite (TFC) membranes. The modification was carried out for PA effective layer by cross-linked PVA layer with different nano-materials. Different modified thin-film nanocomposite (TFNC) membranes were characterized by measuring the contact angle, Attenuated total reflectance–Fourier transform infrared (ATR–FTIR) spectroscopy, X-ray diffraction (XRD), dynamic mechanical analysis (DMA), and scanning electron microscopy (SEM).

2. Experimental

2.1. Material and chemical

The commercial TFC/PA membrane Soultec. Polyvinyl alcohol (99+ % hydrolyzed, with MW 146,000–186,000) was used as received from Sigma-Aldrich (German). Glutaraldehyde (GA), a cross-linking agent, was obtained as a 50% (w/w) aqueous solution ADWIC Chemical Co., (Egypt). Hydrochloric acid 1N standard solution was used as received from Alfa-Aesar Acetone from Alfa-Aesar (United States).

Different nanomaterials were used as zinc oxide nanopowder <100 nm particle size from Sigma-Aldrich. Silica nanoparticles mesoporous 200 nm particle size, pore size 4 nm from Sigma-Aldrich. Titanium dioxide nanopowder <25 nm from Sigma-Aldrich. Multi-walled carbon nanotubes COOH functionalized O.D 10–15 nm, I.D 2–6 nm, length 0.1–10 μm from Sigma-Aldrich. Silver nanoparticle dispersion in ethylene glycol <100 nm from Sigma-Aldrich.

Deionized (DI) water was generated by glass plates were used to support the commercial TFC membranes during surface coating. Additionally, acrylic frames, rubber gaskets having the same size as the acrylic frames. The rocker was used to obtain a homogenous coated layer.

2.2. Modification of thin-film composite membranes

PA/PVA-nano thin-film composite membranes were synthesized via surface coating as follows: commercial PA membranes with dimensions of 20 cm × 20 cm were immersed in DI water for at least 30 min. The membrane was fixed on a glass plate, acrylic ring, and frames were secured to the membrane surface.

A polymer solution of 0.25 wt.% PVA was prepared by dissolving a definite weight of the polymer in DI water with heating at 100°C until obtaining a homogenous solution. PVA solutions were cooled to ambient temperature (25°C) and 2% glutaraldehyde solution in the presence of HCL as a catalyst was placed in the glass ring (in contact with the membrane surface) and constantly stirred with continuous shacking using rocker at ambient conditions. After the desired contact time of the membrane with the PVA solution, the excess solution was drained, the modified membrane was annealed for a certain time at a certain temperature.

For TFNC membranes different types of nanomaterials were used such as zinc oxide, titanium dioxide, silica, CNT-COOH, and silver with a certain concentrations. For TFNC membrane preparation a certain concentration of nanomaterial was sonicated in PVA solution to obtain a homogenous dispersion and added to the membrane surface under the previous condition. Membranes were stored in ultrapure water until characterized or used in Alfa Laval experiments.

2.3. Characterization of modified polyamide-thin film composite (PA-TFC) and (PA-TFNC) membranes

The membranes were characterized by FTIR, XRD, SEM, thermogravimetric analysis (TGA), Mechanical properties, and the contact angle.

ATR–FTIR measurement was carried out to analyze the surface chemistry of uncoated and coated membranes. FTIR analysis was carried out by using FTIR-6300 TYPE A.

XRD was carried out to investigate the nanostructure and crystallinity nature of polymer which carried out by using Xperto PRO.

The microscopic imaging of neat and modified membranes was conducted using a SEM FEI, Quanta 250 FEG (Netherlands) type. Both surface and cross-section samples were tested. The cross-sections membrane samples were prepared by fracturing samples under liquid nitrogen.

The measurements of the static contact angle were conducted by using optical tensiometer KRUSS Model DSA. A water drop was placed onto the membrane surface with a digital microsyringe with a contact angle between the water and the membrane measured when no further change was observed. The measurements were performed in the open air and the results are given as an average of three parallel measurements.

Thermal gravimetric analysis was carried out using a Shimadzu TGA system (TGA-30).

The mechanical properties of the membrane samples were measured with Universal Testing Instruments (DMA-Q 860), where the dynamic strain and stress were measured at room temperature (25°C). Tensile tests were carried out to assess Young's modulus and strain at fracture of samples at the rate of 10 mm/min. The membrane samples were cut into rectangles with a dimension of 20 mm × 13 mm × 0.15 mm, and fixed perpendicular to one another in between two automatic gripping units of the sample, leaving a 3 cm sample extent for mechanical loading. The thickness of the membrane samples was determined with an automatic micrometer with a precision of 1 μm. Young's modulus (Megapascal, Mpa) was calculated using the following equation:

$$\text{Young's modulus}\left(\text{Mpa}\right)=\frac{\text{stress}}{\text{strain}} \tag{1}$$

2.4. Performance and evaluation of modified RO membranes

Reverse osmosis performance for modified TFC membranes was conducted using the laboratory reverse osmosis system, model LAB-20, manufactured by the Danish Sugar Corp., Ltd., Denmark. It consists of a stainless steel cylindrical vessel, 20 cm in diameter, and 70 cm high. The minimum number of membranes that can be used is 2 and the maximum is 20. The effective membrane area is 0.018 m^2. The membrane performance evaluated through measuring both permeate flux (L m^{-2} h^{-1}) and salt rejection (%) using an aqueous feed solution contained 2,000 ppm NaCl with pH range 7 ± 0.2 at 25°C at 15 bar applied pressure All flux and salt rejection (%) measurements were evaluated after 15 min for 3 h from the starting to ensure that the filtration process had reached the steady-state.

The permeate flux (JW) through a membrane area (A) was calculated as the volume (ΔV) collected during a time period Δt:

$$\text{JW}=\frac{\Delta V}{A}\Delta t \tag{2}$$

Also, the salt rejection (R_s %) was calculated by measuring the electric conductivity of both feed and permeate

solutions using a conductivity meter. The salt rejection percent (R_S %) was calculated as follows:

$$R_s\% = \left(\frac{C_f - C_p}{C_f}\right) \times 100 \quad (3)$$

where C_f and C_p are the concentrations of the feed and permeate water (product), respectively [17].

The oil/water emulsion was prepared by blending 4.5 g Triton-X surfactant and 40.5 g soybean oil in 3 L of water using an industrialized blender for 3 min at the blender's highest speed. This mixture was then diluted to a total volume of 30 L using ultra-pure water (the final concentration was 1,500 ppm with a total organic carbon concentration of 40,000 ppm). This emulsion was applied in order to determine their fouling resistance through total organic carbon measurement.

3. Results and discussion

3.1. Characterization of membranes

Characteristic of modified membrane with several nano-materials was studied and discussed.

3.1.1. FTIR spectroscopy

FTIR spectroscopy was made for the different modified membranes included TFC/PVA-TiO_2, TFC/PVA-Ag, TFC/PVA-ZnO, TFC/PVA-CNT, TFC/PVA-Si. The purpose of FTIR spectroscopy is to examine the presence of functional groups present in the skin surface layer of membrane samples.

For TFC/PVA-ZnO membrane, as shown in Fig. 2, new intense broadband between 500 and 850 cm^{-1} assigned to the Zn–O vibration of ZnO which appeared and indicated the presence of ZnO nanoparticles that dopped in PVA solution on the surface [18].

For TFC/PVA-Si membrane, Silica shows characteristic peaks at 1,006; 848; and 439 cm^{-1} corresponding to the asymmetrical stretching, symmetric stretching, and bending vibrations in Si–O–Si bonds, respectively [19].

For TFC/PVA-TiO_2 membrane a strong broad absorption band at 3,463 cm^{-1} were observed and assigned to Ti–OH. This absorption wide band arised due to the hydrogen bonding between OH of PVA molecules with the titanium ions Ti^+ and allowed forming a charge transfer complex. These charge-transfer complexes suggest that the number of charges must increase with increasing TiO_2 [20].

For TFC/PVA-Ag membrane the band at 1,420 cm^{-1} indicates decoupling between the corresponding vibrations due to interaction between the Ag nanoparticles and the O–H groups originating from the PVA chains [21].

For TFC/PVA-COOH-CNT membrane, two bands were observed at 3,459 and 2,973 cm^{-1} attributed to COOH coming during the functionalization of CNTs. Also, a new band at 1,650 cm^{-1} is attributed to C–C band between CNTs and PVA. The appearance of this band might be the signature for the interaction of *p*-bonds at the surface of CNTs with the open double band on PVA [22].

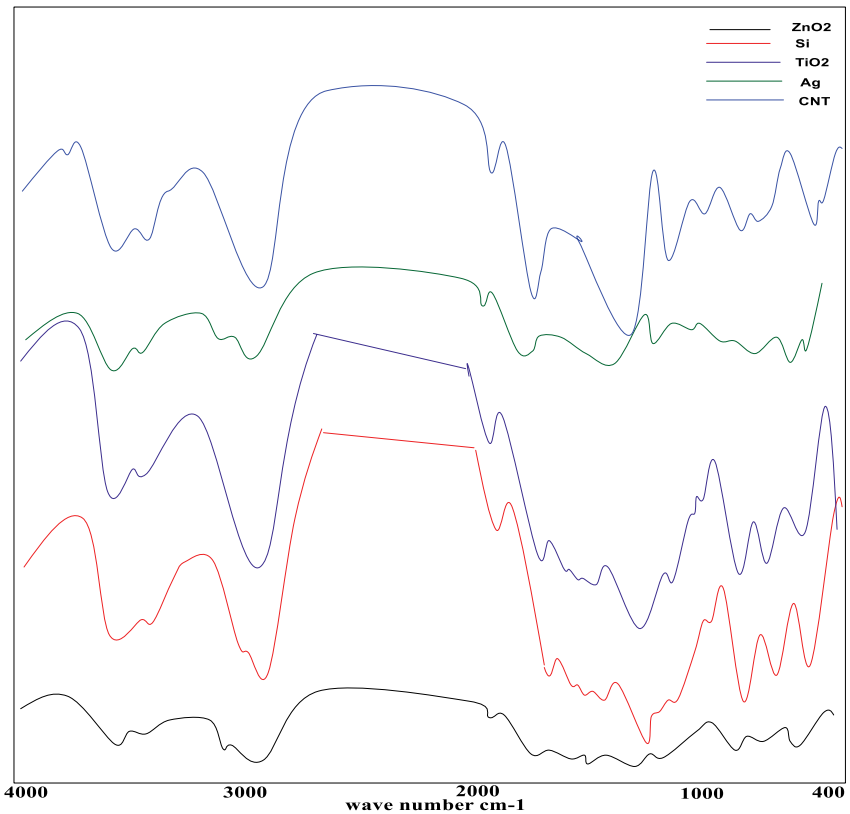

Fig. 2. FTIR of different modified membranes with PVA and different nano-materials.

3.2. Scanning electron microscopy

The SEM characterization was performed to determine the PVA coated layer thickness and to verify how the coated layers were formed on a different membrane. The surface morphology of different modified membranes; TFC/PVA-ZnO, TFC/PVA-Si, TFC/PVA-TiO_2, TFC/PVA-Ag, and TFC/PVA-CNT were examined by SEM as shown in Fig. 3.

3.3. X-ray diffraction

As shown in Fig. 4 for TFC/PVA-TiO_2, two additional peaks at around 26° and 32.8° attributable to anatase and rutile TiO_2, respectively. This demonstrates that TiO_2 nanoparticles are strongly bounded in the PA membranes due to specific interaction of TiO_2 with PA and the in-situ interfacial polymerization method. Two types of interaction were proposed: (1) coordination interaction between Ti atoms and carboxylic groups and (2) hydrogen bonding between the surface hydroxyl group of TiO_2 and carbonyl group [23].

Change of peak intensity has been found in the samples doped CNTs indicating a complete dissociation of CNTs in the polymer matrix Fig. 8. In general, the crystalline nature of PVA was detected from the strong interaction between PVA through intermolecular hydrogen bonding. An interaction between PVA with carboxylic groups (COOH) in CNTs led to a decrease in the intermolecular interaction of PVA chains, which results in the decrease in a degree of PVA-crystalline. The new peak corresponding to different crystal planes which indicates the reflections that correspond to CNTs at a 2θ = 26.44 was observed. This peak is corresponding to the reflection of the hexagonal crystal structure of graphite [22].

The XRD pattern of the prepared TFC/PVA-Ag nanocomposite additional peaks at 2θ value of about 42.5°, as shown in Fig. 4. This confirmed the crystalline nature of Ag nanoparticles [24].

A new peak is seen at an angle of 21.8° (*d* spacing of 4.07 Å) which was not observed in the PVA pattern due to the exfoliated silica nanoparticles dispersed in the PVA matrix [25].

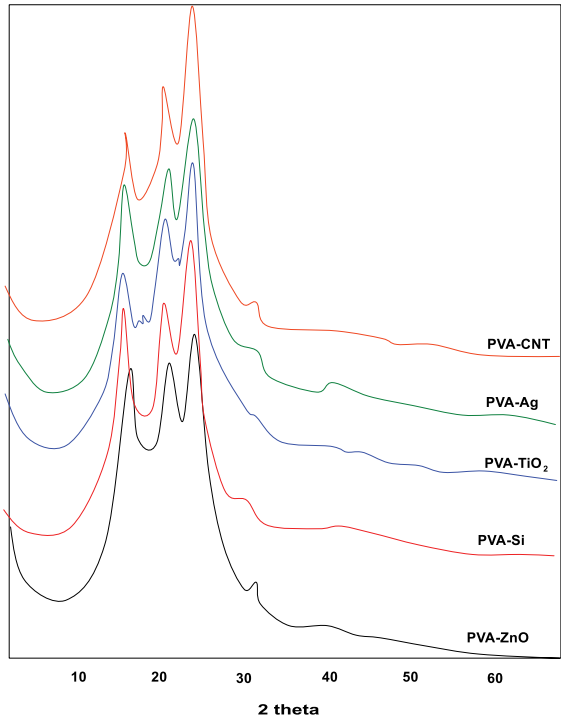

Fig. 4. XRD spectra for PVA-CNT, PVA-Ag, PVA-TiO_2, PVA-Si, PVA-ZnO.

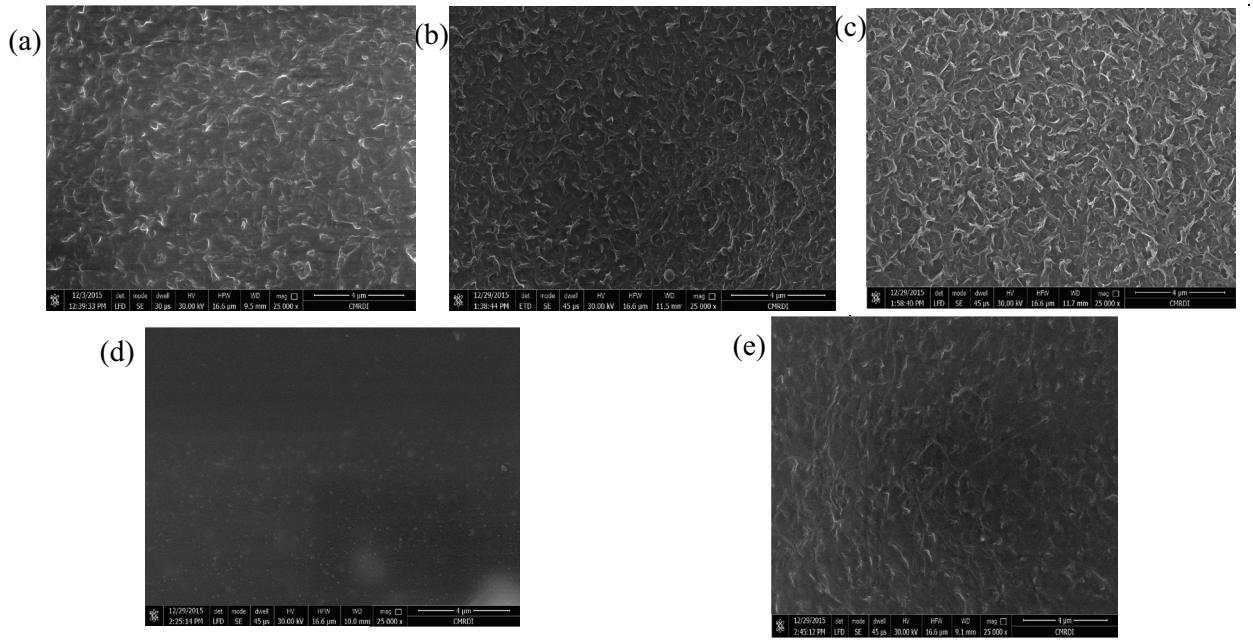

Fig. 3. SEM image of (a) TFC/PVA-Zno, (b) TFC/PVA-Si, (c) TFC/PVA- TiO_2, (d) TFC/PVA-Ag, and (e) TFC/PVA-CNT.

3.4. Thermal analysis

TGA of TFC/PVA-TiO_2, TFC/PVA-Ag, TFC/PVA-ZnO, TFC/PVA-CNT, and TFC/PVA-Si polymer nanocomposites are shown in Fig. 5. The degradation rate of the nanocomposite is significantly lower. Under a given heating rate, the TGA curve of the nanocomposite is situated at a higher temperature than that of the pure PVA [26].

The degradation of TFC/PVA-ZnO occurs in one step at temperature range 300°C to 650°C with mass change 97.4% and total mass loss (–1.168 mg) which can be explained as The peaks around 300°C corresponds to the loss of water which form H bond between PVA molecules. The two exothermic peaks at about 350°C and 550°C are associated with the degradation of side-chain (the scission of C–O) and main chain (the scission of C–C The above results demonstrate the existence of some interactions between a PVA molecule and ZnO via forming H bond and an O–Zn–O bond [18,27].

Due to the presence of SiO_2, the TGA curves of the nanocomposite shift to higher degradation temperature range 300°C–700°C with mass change 99% and total mass loss (–3.43 mg) [26]. These results suggest that the introduction of silica into the PVA chains enhances the thermal stability of the given nanocomposite materials, which may be attributed to the high thermal stability of silica and the nature of the crosslinking network between the silica phase and PVA bulk [28].

The PVA-TiO_2 composite exhibits two-stage continuous decomposition takes place up to 400°C which may be due to PVA present in the composite exhibiting around 85% weight loss in this temperature range. A gradual decomposition was noticed after 400°C continuing up to 600°C followed by a plateau region with a constant weight at 600°C (around 28%). The composites of TiO_2, however, exhibit hardly any residue at 600°C. It may be due to the oxidative decomposition of carbonaceous mass (formed during the degradation of polymer chains) by TiO_2 after 400°C. All these observations clearly indicate that the thermal decomposition mechanism is different for PVA and for its composite with TiO_2. The marginal improvement in thermal stability of PVA is indicated by a shift in its decomposition temperature to the higher side as mentioned. The increase in the thermal stability can be explained in terms of interaction of titanium with the oxygen of the secondary hydroxyl group of PVA forming a complex. It may affect the heat transfer process from one polymer chain to other and thus needs more thermal energy for further decomposition resulting an increase in decomposition temperature [29].

For TFC/PVA-Ag nanocomposite An improvement in the thermal stability of the nanocomposite can be seen in which thermal degradation is shifted to higher temperatures up to 400°C with mass change 99% and total mass loss (–1.6 mg). The degradation of polymers starts with free radical formations at weak bonds and/or chain ends, followed by their transfer to adjacent chains via inter-chain reactions. The improved thermal stability can be explained through the reduced mobility of the PVA chains in the nanocomposite. Because of reduced chain mobility, the chain transfer reaction will be suppressed, and consequently the degradation process will be slowed and decomposition will take place at higher temperatures. It is important to point out that the residual weight of the nanocomposite is more than one order of magnitude larger than the content of the inorganic phase at 600°C, while at the same temperature the pure PVA is completely decomposed. This result indicates that the thermal decomposition routes of the pure PVA and the PVA-Ag nanocomposites are different [21].

The PVA-CNT composite exhibits thermal decomposition at two stages at 420°C and 620°C resulting mass change of 70.9% and 27.8% with total mass loss (–4.94 mg), where at high temperature, CNT undergo structural changes that have been studied to elucidate the mechanisms of decomposition [30].

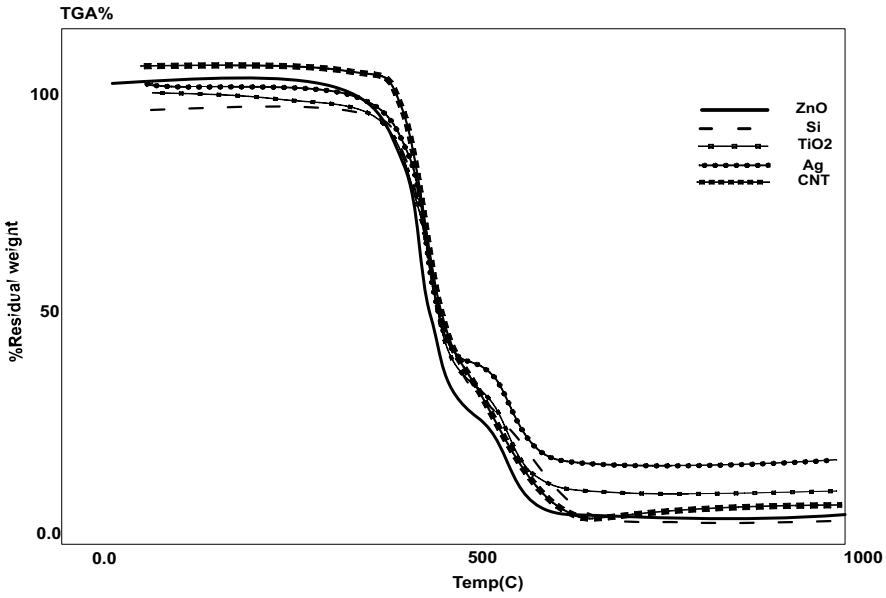

Fig. 5. TGA spectra for PVA-CNT, PVA-Ag, PVA-TiO_2, PVA-Si, and PVA-ZnO.

3.5. Contact angle

The results of contact angle measurement are presented in Table 1 and show the neat TFC membrane has the highest contact angle of 65.6°, corresponding to the lowest surface hydrophilicity.

Modification by adding nanoparticles to increase surface hydrophilicity may be due to a greater attraction of water molecules by the nanoparticles.

3.6. Mechanical properties

Various mechanical properties were determined for PVA/ZnO, PVA/TiO_2, PVA/CNT-COOH, PVA/Si, PVA/Ag, and unmodified. Data on the various properties are included in Table 2.

It can be seen from the table that the mechanical properties of the PVA/ZnO membrane have been enhanced causing increased strength and flexibility. The addition of ZnO to the membrane makes it more crystalline, and the crystalline membrane is stronger than the amorphous ones [31].

There is a significant increase in the tensile strength of PVA/TiO_2 in comparison with neat TFC/PVA. The increase in tensile strength may be due to the homogenous dispersion of nano-TiO_2 clusters and the interfacial interaction of titanium with hydroxyl groups of the PVA. Elongation was found to decrease due to the stiffness of nano-TiO_2 [29].

Tensile strength of PVA/CNT-COOH increase in comparison with neat PVA. Such an increase was attributed to cross-linking between COOH on nano-TiO_2 surface and OH of the PVA chain.

Table 1
Contact angle measurement for PVA-CNT, PVA-Ag, PVA-TiO_2, PVA-Si, PVA-ZnO

Membrane type	Contact angle (°)
Uncoated TFC	65.6
PA/PVA-ZnO	51 ± 0.1
PA/PVA-Si	55 ± 0.3
PA/PVA-TiO_2	53 ± 0.1
PA/PVA-Ag	50 ± 0.1
PA/PVA-CNT	56 ± 0.3

Table 2
Mechanical properties for PVA-CNT, PVA-Ag, PVA-TiO_2, PVA-Si, PVA-ZnO

Membrane type	Tensile strength (M Pa)	Maximum elongation (%)
Neat TFC	29.9	0.86
PVA/ZnO	23.3	6.14
PVA/Si	11.2	0.67
PVA/TiO_2	25.09	3.5
PVA/Ag	29.8	3.12
PVA/CNT-COOH	29.8	2.32

Silver nanoparticles affect the structural rearrangements during the post-elastic deformation to induce a semi-crystalline which leads to increase tensile strength. Also silver nanoparticles have high modulus that's because of high bulk to surface ratio of the particles as well as the attachment of PVA chains to their surface. Because of the attachment of polymer segments, the transfer of mechanical energy from the matrix to the high-modulus filler will be significantly enhanced, that is, the modulus of the material as a whole increases [21].

Silica nanocomposite membrane has a low tensile strength, this is may be due to the decrease of molecular mobility of particle and there is interaction with PVA polymer. This result was an agreement with the previous work [25].

4. Performance evaluation of modified RO membranes

Reverse osmosis performance for the synthesized modified TFC membranes was conducted using the laboratory Reverse osmosis system. The effect of surface coatings on the membrane performance was studied through the measuring of both salt rejection and water flux measurement for a feed solution of 2,000 mg/L NaCl at the applied pressure of 15 bar and an ambient temperature of 25°C for 3 h operation time.

A series of PVA/TiO_2 nanocomposite membranes were prepared under the specified conditions using three different TiO_2 concentrations; 0.5, 1, and 2 wt.% of PVA concentration.

The effect of TiO_2 concentration on the salt rejection of the membranes was shown in Fig. 6. It is obvious that, there was an increase in both salt rejection (%) and water flux with increasing the concentration of TiO_2. This increase in salt rejection occurred due to the deposition of TiO_2 nanoparticles on the surface of the PVA/PA membrane that might plug any pinholes and local defects, and thus enhances the salt rejection, this result was an agreement with the previous work of [32].

The effect of ZnO concentration on both the salt rejection and the water flux for the membranes is shown in Fig. 7. The result showed that 1% of ZnO is the applicable concentration which gives the higher salt rejection and water flux than the un-modified TFC membrane.

The effect of silver concentration on the salt rejection and water flux of the membranes was studied under the specified conditions at different nano silver concentrations as (0.5%,1%, and 2%)of polymer concentration is shown. The result illustrated in Fig. 8 show decreasing both salt rejection and water flux with increasing silver concentration.

Effect of change silica concentration on salt rejection and water flux shown in Fig. 9.

The result has shown the most applicable concentration is 1% because at higher content of silica particle the depletion of hydrophilic hydroxyl groups increases led to these nanocomposite membranes exhibiting lower sorption selectivity for water [28]. The effect of silica concentration on water flux. By increasing silica concentration water flux increase because of increased hydrophilicity of the membrane surface.

The effect of CNT concentration on the salt rejection and water flux of the membranes is shown in Fig. 10. The results show increasing both salt rejection and water flux with increasing concentration of CNT.

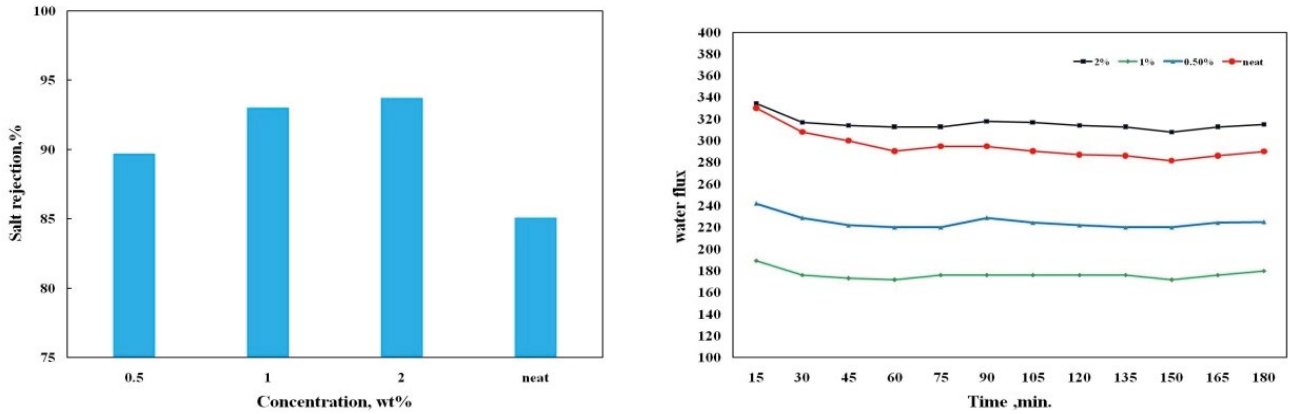

Fig. 6. Effect of TiO_2 concentration on a salt rejection and water flux of modified membranes.

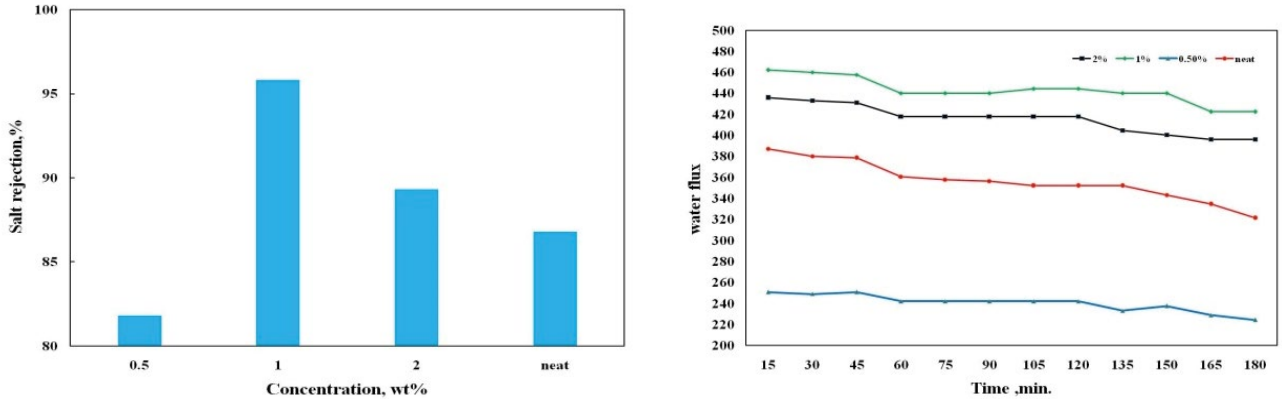

Fig. 7. Effect of ZnO concentration on a salt rejection and water flux of modified membranes.

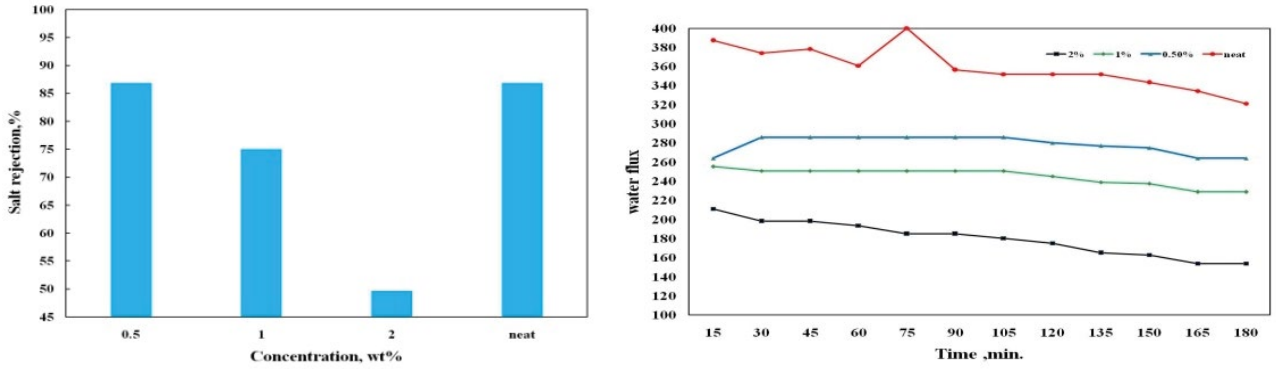

Fig. 8. Effect of Ag concentration on a salt rejection and water flux of modified membranes.

5. Emulsified oil fouling analysis

The fabricated membranes have been tested using the reverse osmosis pilot-scale laboratory unit (Unitmodel LAB-20) to investigate the membrane efficiency for organic matter removal and their fouling resistance. The oil/water emulsion was used as a feed source in the RO pilot-scale unit using the neat and different modified membranes such as; TFC/PVA, TFC/PVA-Si, TFC/PVA-TiO_2, TFC/PVA-Ag, TFC/PVA-ZnO, and TFC/PVA-CNT-COOH.

By measuring the concentration of total organic carbon during the water desalination processes of neat and modified selected membranes for 25 h, as shown in Table 3, it was found that after 25 h, by using the different modified membranes, there was a complete remove of organic matter. On the other hand, there was only 50% remove by using the neat membrane.

Also, the fouling experiment was carried out using the selected membranes 25 h using an applied pressure

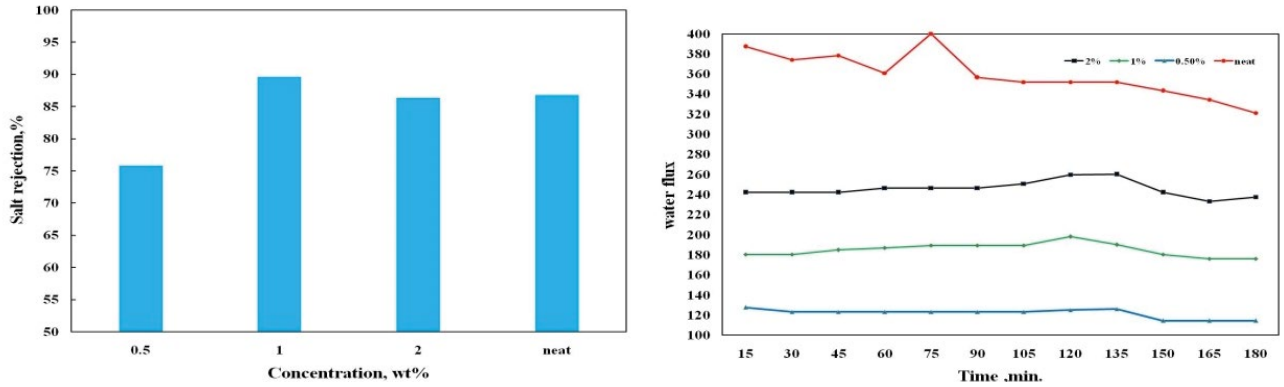

Fig. 9. Effect of Si concentration on a salt rejection of modified membranes.

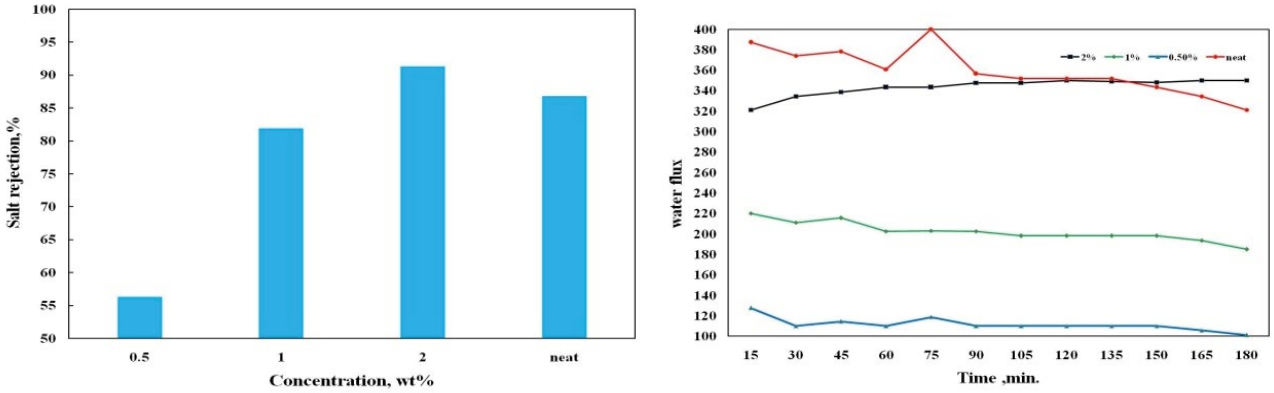

Fig. 10. Effect of CNT concentration on a salt rejection and water flux of modified membranes.

Table 3
Total organic carbon concentration of neat and different modified membranes

	5 h	10 h	15 h	20 h	25 h
Neat TFC	40,000	30,000	20,000	20,000	20,000
Modified TFC/PVA	Nil	Nil	Nil	Nil	Nil
TFC/PVA-ZnO	10,000	10,000	10,000	10,000	Nil
TFC/PVA-Si	Nil	Nil	Nil	Nil	Nil
TFC/PVA-TiO_2	10,000	10,000	Nil	Nil	Nil
TFC/PVA-Ag	Nil	Nil	Nil	Nil	Nil
TFC/PVA-CNT-COOH	40,000	10,000	Nil	Nil	Nil

of 15 bar, as shown in Fig. 11. The permeate of each membrane was collected and measured both water flux and salt rejection (%). Table 4 shows the salt rejection of modified selected membranes in comparison with neat TFC membranes. Fig. 11 shows an improvement in both water flux and fouling resistance of modified selected membranes than that of the neat membrane by the following sequence:

For permeate flux: TFC/PVA-ZnO > Modified TFC/PVA > TFC/PVA-TiO_2 > TFC/PVA-Si > TFC/PVA-Ag > TFC/PVA-CNT > Neat TFC

For salt rejection: Modified TFC/PVA > TFC/PVA-Ag > TFC/PVA-ZnO > TFC/PVA-TiO_2 > TFC/PVA-Si > TFC/PVA-CNT

Table 4
Salt rejection of neat TFC and different modified membranes

Membrane type	Salt rejection (%)
Uncoated TFC	56.2
PVA coated TFC	93.5
PA/PVA-ZnO	78
PA/PVA-Si	69.4
PA/PVA-TiO_2	71.7
PA/PVA-Ag	89
PA/PVA-CNT	62.7

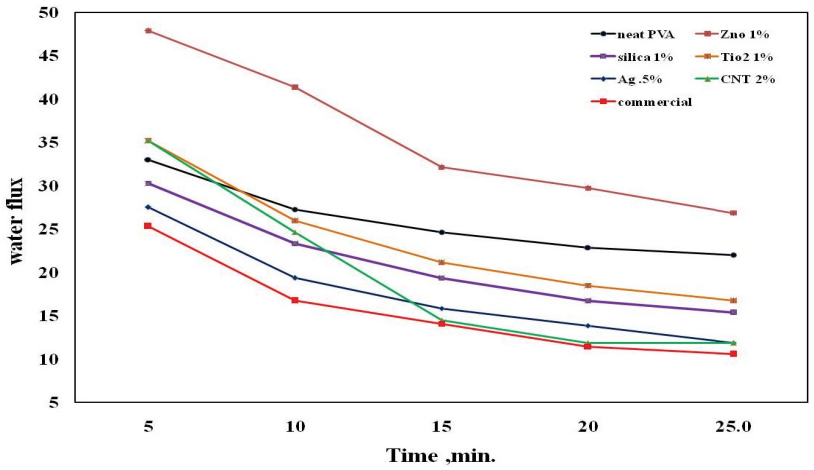

Fig. 11. Fouling behavior during oil/water emulsion of modified and uncoated membranes.

6. Conclusions

Surface modification has been attempted to improve the membrane properties of the commercial thin-film composite membrane. The modification was obtained through surface coating using PVA with different types of nanomaterials. By surface modification, the membrane surface properties were improved and the membranes become more fouling resistance through enhanced surface hydrophilicity.

The salt rejection improved from 82% to 95% with continuous water flux with completely remove the organic matter.

Acknowledgment

The author thanks the Egyptian Scientific Technology Development Funding (STDF) for technical support and for funding of the project.

References

[1] U.S. Department of the Interior Desalination Research and Development Program, Bureau of Reclamation, P.O. Box: 25007, Denver Federal Center.
[2] G.D. Kang, Y.M. Cao, Development of antifouling reverse osmosis membranes for water treatment: a review, Water Res., 46 (2012) 584–600.
[3] C.Y. Tang, T.H. Chong, A.G. Fane, Colloidal interactions and fouling of NF and RO membranes: a review, Adv. Colloid Interface Sci., 164 (2011) 126–143.
[4] A.-H.M. El-Aassar, Improvement of reverse osmosis performance of polyamide thin-film composite membranes using TiO_2 nanoparticles, Desal. Water Treat., 55 (2015) 2939–2950.
[5] B.J.A. Tarboush, D. Rana, T. Matsuura, H.A. Arafat, R.M. Narbaitz, Preparation of thin-film-composite polyamide membranes for desalination using novel hydrophilic surface modifying macromolecules, J. Membr. Sci., 325 (2008) 166–175.
[6] D. Rana, T. Matsuura, R.M. Narbaitz, Novel hydrophilic surface modifying macromolecules for polymeric membranes: polyurethane ends capped by hydroxy group, J. Membr. Sci., 282 (2006) 205–216.
[7] S.H. Kim, S.Y. Kwak, B.H. Sohn, T.H. Park, Design of TiO_2 nanoparticle self-assembled aromatic polyamide thin-film-composite (TFC) membrane as an approach to solve biofouling problem, J. Membr. Sci., 211 (2003) 157–165.
[8] N. Kim, D.H. Shin, Y.T. Lee, Effect of silane coupling agents on the performance of RO membranes, J. Membr. Sci., 300 (2007) 224–231.
[9] V. Freger, J. Gilron, S. Belfer, TFC polyamide membranes modified by grafting of hydrophilic polymers: an FT-IR/AFM/TEM study, J. Membr. Sci., 209 (2002) 283–292.
[10] G. Chen, S.H. Li, X.S. Zhang, S.B. Zhang, Novel thin-film composite membranes with improved water flux from sulfonated cardo poly(arylene ether sulfone) bearing pendant amino groups, J. Membr. Sci., 310 (2008) 102–109.
[11] A. Kulkarni, D. Mukherjee, W.N. Gill, Flux enhancement by hydrophilization of thin-film composite reverse osmosis membranes, J. Membr. Sci., 114 (1996) 39–50.
[12] D. Mukherjee, A. Kulkarni, W.N. Gill, Chemical treatment for improved performance of reverse osmosis membranes, Desalination, 104 (1996) 239–249.
[13] H. Wu, B. Tang, P. Wu, Novel ultrafiltration membranes prepared from a multi-walled carbon nano tubes/polymer composite, J. Membr. Sci., 362 (2010) 374–383.
[14] D.J. Miller, P.A. Araujo, P.B. Correia, M.M. Ramsey, J.C. Kruithof, M.C.M.van Loosdrecht, B.D. Freeman, D. Paul, M. Whiteley, J.S. Vrouwenvelder, Short-term adhesion and long-term biofouling testing of polydopamine and poly(ethylene glycol) surface modifications of membranes and feed spacers for biofouling control, Water Res., 46 (2012) 3737–3753.
[15] K. Lang, S. Sourirajan, T. Matsuura, G. Chowdhury, A study on the preparation of polyvinyl alcohol thin-film composite membranes and reverse osmosis testing, Desalination, 104 (1996) 185–196.
[16] M.A. Elharati, Poly(vinyl alcohol)/Polyamide Thin-Film Composite Membranes, Thesis Presented in Partial Fulfillment of the Requirements for the Degree of Master of Science in Engineering (Chemical Engineering) at Stellenbosch University, 2009.
[17] A.M. El-Aassar, Polysulfone/polyvinyl alcohol thin-film nanocomposite membranes: synthesis, characterization and application for desalination of saline groundwater, J. Appl. Sci. Res., 8 (2012) 3811–3822.
[18] X.M. Sui, C.L. Shao, Y.C. Liu, White-light emission of polyvinyl alcohol ZnO hybrid nanofibers prepared by electrospinning, Appl. Phys. Lett., 87 (2005) 113115.
[19] T. Pirzada, S.A. Arvidson, C.D. Saquing, S.S.A. Khan, Hybrid silica–PVA nanofibers via sol–gel electro spinning, Am. Chem. Soc., Langmuir, 28 (2012) 5834–5844.
[20] A.M. Shehap, D.S. Akil, Structural and optical properties of TiO_2 nanoparticles/PVA for different composites thin-films, Int. J. Nano-electronics and Materials, 9 (2015) 17–36.
[21] Z.H. Mbhele, M.G. Salemane, C.G.C.E. van Sittert, J.M. Nedeljkovic, V. Djokovic, A.S. Luyt, Fabrication and characterization of silver-polyvinyl alcohol nanocomposites, Chem. Mater., 15 (2003) 5019–5024.

[22] N.S. Alghunaim, Optimization and spectroscopic studies on carbon nanotubes/PVA nano-composites, Results Phys., 6 (2016) 456–460.
[23] H.S. Lee, S.J. Im, J.H. Kim, J.P. Kim, B.R. Min, Polyamide thin-film nanofiltration membranes containing TiO_2 nanoparticles, Desalination, 219 (2008) 48–56.
[24] M. DeviJ, M. Umadevi, Synthesis and characterization of silver–PVA nanocomposite for sensor and antibacterial applications, J. Cluster Sci., 25 (2014) 639–650.
[25] M. Bhattacharya, S. Chaudhry, High-performance silica nanoparticle reinforced poly(vinyl alcohol) as templates for bioactive nanocomposites, Mater. Sci. Eng., C, 33 (2013) 2601–2610.
[26] Z. Peng, L.X. Kong, A thermal degradation mechanism of polyvinyl alcohol/silica nanocomposites, Polym. Degrad. Stab., 92 (2007) 1061–1071.
[27] M.M. Ali Khan, Rafiuddin, Inamuddin, PVC based polyvinyl alcohol zinc oxide composite membrane: synthesis and electrochemical characterization for heavy metal ions, J. Ind. Eng. Chem., 19 (2013) 1365–1370.
[28] R. Guo, X. Ma, C. Hu, Z. Jiang, Novel PVA–silica nanocomposite membrane for pervaporative dehydration of ethylene glycol aqueous solution, Polymer, 48 (2007) 2939–2945.
[29] R. Singh, S.G. Kulkarni, S.S. Channe, Thermal and mechanical properties of nano-titanium dioxide-doped polyvinyl alcohol, Polym. Bull., 70 (2013) 1251–126.
[30] J.H. Lehman, M. Terrones, E. Mansfield, K.E. Hurst, V. Meunier, Evaluating the characteristics of multiwall carbon nanotubes, Carbon, 49 (2011) 2581–2602.
[31] H. Isawi,M.H. El-Sayed, X. Feng, H. Shawky, M.S. Abdel-Mottaleb, Surface nanostructuring of thin-film composite membranes via grafting polymerization and incorporation of ZnO nanoparticle, Appl. Surf. Sci., 385 (2016) 268–281.
[32] S. Pourjafar, A. Rahimpour, M. Jahanshahi, Synthesis and characterization of PVA/PES thin-film composite nanofiltration membrane modified with TiO_2 nanoparticles for better performance and surface properties, J. Ind. Eng. Chem., 18 (2012) 1398–1405.